MASSACHUSETTS INSTITUTE OF TECHNOLOGY

HAYSTACK OBSERVATORY
WESTFORD, MASSACHUSETTS 01886
2 December 1993

Telephone: 508-692-4764
Fax: 617-981-0590

To: Millimeter-wave VLBI Group

From: Alan E.E. Rogers AEER

Subject: "Double-Dicke" beam switched spectral baseline stability: Theory and Measurements

On the radome-enclosed Haystack antenna, the dominant sources of baseline ripple are multi-path to the subreflector and multi-path to the radome panels. (Multi-path to the shadowed annulus of the main reflector having been eliminated by a large spoiler.) In either case, the ripple is the result of a combination of the internal noise of the "Weinreb" effect and antenna noise being transmitted back out of the feed for an additional path of 76.8′ (12.8 MHz) to the subreflector and 110′ (9 MHz) to the radome and back. A shorter multiple path is the result of reflections from the front-end back to the front of the feed which is canceled along with the receiver bandpass in the difference between the signal and comparison cycles of the beam switch provided the antenna signal levels are well balanced.

Since the subreflector and radome reflections are different for the main and offset beams they do not cancel in the first difference of the beam switch and a second difference ("double-Dicke") is needed. In the double-Dicke difference the baseline ripple magnitude B is approximately

$$B = T\left(n_s - n_r\right)\left(S + b\right) + A_s\left(R\left(\theta_s\right) - R\left(\theta_r\right)\right) + \left(g\left(\theta_s\right) - g\left(\theta_r\right)\right)$$

where
- A_s = antenna temperature
- $(n_s - n_r)$ = unbalance in beam switching efficiency
- T = source temperature
- S = subreflector reflection $\approx 10^{-3}$ without absorber or spoiler; $\approx 10^{-4}$ with spoiler
- $R(\theta)$ = radome reflection as a function of antenna pointing $\approx 5 \times 10^{-5}$ at 115 GHz
- b = receiver ripple (from many causes) $\approx 10^{-2}$ for 3mm SIS
- $g(\theta)$ = ground scatter as a function of antenna pointing

Both of the first two terms can be a limiting factor in spectral line and the third limits continuum measurements. Any unbalance or atmospheric temperature variations can result in the subreflector and receiver ripple appearing in the average of many double-Dicke cycles. In this regard it is advantageous to reduce the subreflector reflection at 115 GHz as much as possible. While radome reflections are small at 115 GHz they do not cancel in the first or second difference. The angular scale for radome reflections is about 50 mdeg at 115 GHz compared with 1500 mdeg scale for ground scatter from the radome. Many double-Dicke cycles can be used to reduce the radome effects which are pseudo-random. For example, if $A_s \approx 100$K and $R \approx 5 \times 10_{-s}$ then in one double-Dicke cycle (of short integration) the residual radome ripple is $\approx 10mK$. Over many cycles or during an integration during which the angle changes, the residual ripple will be reduced by the square root of the number of independent cycles. Alternately a radome retrace can be used for comparison but since there is no signal present during the retrace, four times more integration is needed to achieve the same SNR.

Ground scatter angular scale size

Meeks and Ruze studied variation of ground scatter ("noise granularity") with antenna pointing and estimated variations of 0.015 ($\approx$0.5K at 115 GHz) with an approximate scale of 1.5 degrees. This scatter should be extremely broadband since it does not involve any multi-path. It may, however, produce a baseline slope of order, *5mK*/GHz. The ground scatter granularity limits the continuum sensitivity and makes radome retrace essential for continuum observations.

The last term in the approximate expression for the ripple magnitude is the term which accounts for the change in ground scatter with antenna position. For continuum this term may be dominant while for spectral line it will only contribute a small slope. Since the switched beams for the 3mm receiver are only 0.128 degrees apart the ground scatter unbalance will only be a fraction *($\approx$ (0.128/1.5) $\approx$ 40 mK)* of the total ground scatter variation with angle for a single feed total power system. This term could be further reduced by having the beams of a switched system as close as possible.

Radome reflection angular scale size

Radome reflections occur primarily at those panels which are just outside the edge of the subreflector and subtend an angle of about 7 degrees. A pointing change of about 0.05 degrees will produce a quarter wavelength path length change to these panels at 115 GHz.

MEASUREMENTS

Subreflector reflections

Figure 1 shows the subreflector reflection ripple. The observed magnitude is about 1K peak-to-peak without spoiler. The period is consistent with the multipath being from the SIS mixer to the subreflector and back.

Figure 2 shows the reduction in ripple when a 10" diameter absorber is placed in the center of the subreflector.

"Lens-Cap" or receiver ripple

Figure 3 shows the baseline ripple where frequency switching with a cap over the receiver feed. This large ripple is thought to be due to multiple reflections inside the SIS mixer dewar. The ripple pattern is dependent on the r.f. frequency and shifts when the first L.O. frequency is changed. The "lens cap" ripple is evident, at a lower level, when the feed is covered by an absorber and is evident whenever there is an unbalance in the beam switched power. The residual ripple in Figure 2 is probably "lens cap" ripple. Even with balanced power in the beam switch, there are reflections from the beam switch wheel which depend on switch phase. These produce ripple which cancel in the double difference.

Radome reflections

Radome reflections are expected to result in a ripple amplitude of about 15 mK at 115 GHz and 150 mK at 86 GHz. Figure 4 shows the baseline ripple at 90 and 95 degrees azimuth. The difference due to radome reflections is about 100 mK. More measurements are needed to confirm this result. In addition, the angular correlation scale needs to be measured.

Double beam "double-Dicke"

Figure 5 shows the baseline for 20 pairs of subspectra each taken with beam switching in which the main and offset beams are placed on the source by position switching the antenna. The measured rms baseline ripple is in good agreement with the theoretical rms. Longer integrations are needed to determine the ultimate limits of baseline performance.

– NORMAL – BEAM SW.

32; 1 AZEL CO 1–0 HAYSTACK 120 O: 12–NOV–1993 R: 12–NOV–199

RA: 17:42:29.370 DEC: –28:59:18.20 (1950.0) Offs: 0.0 0.0 Eq

Unknown Tau: 0. Tsys: 789.1 Time: 3.000 El: 45.00

N: 8192 I0: 4097. V0: 0. Dv: 5.0796E–02 LSR

F0: 115271.200 Df: –1.9531E–02 Fi: 0.

B ef: 0. F ef: 1.0413E–02 G im: 0.

H2O : 0. Pamb: 0. Tamb: 0.0 Tchop: 0.0 Tcold: 0.0

Tatm: 0.0 Tau: 0. Tatm i: 0.0 Tau i: 0.

******

50 mils = $\lambda/2$ = 360°

25 mils = $\lambda/4$ = 180°

12.5 mils = $\lambda/8$ = 90°

λ = 2.6 mm = 103 mils

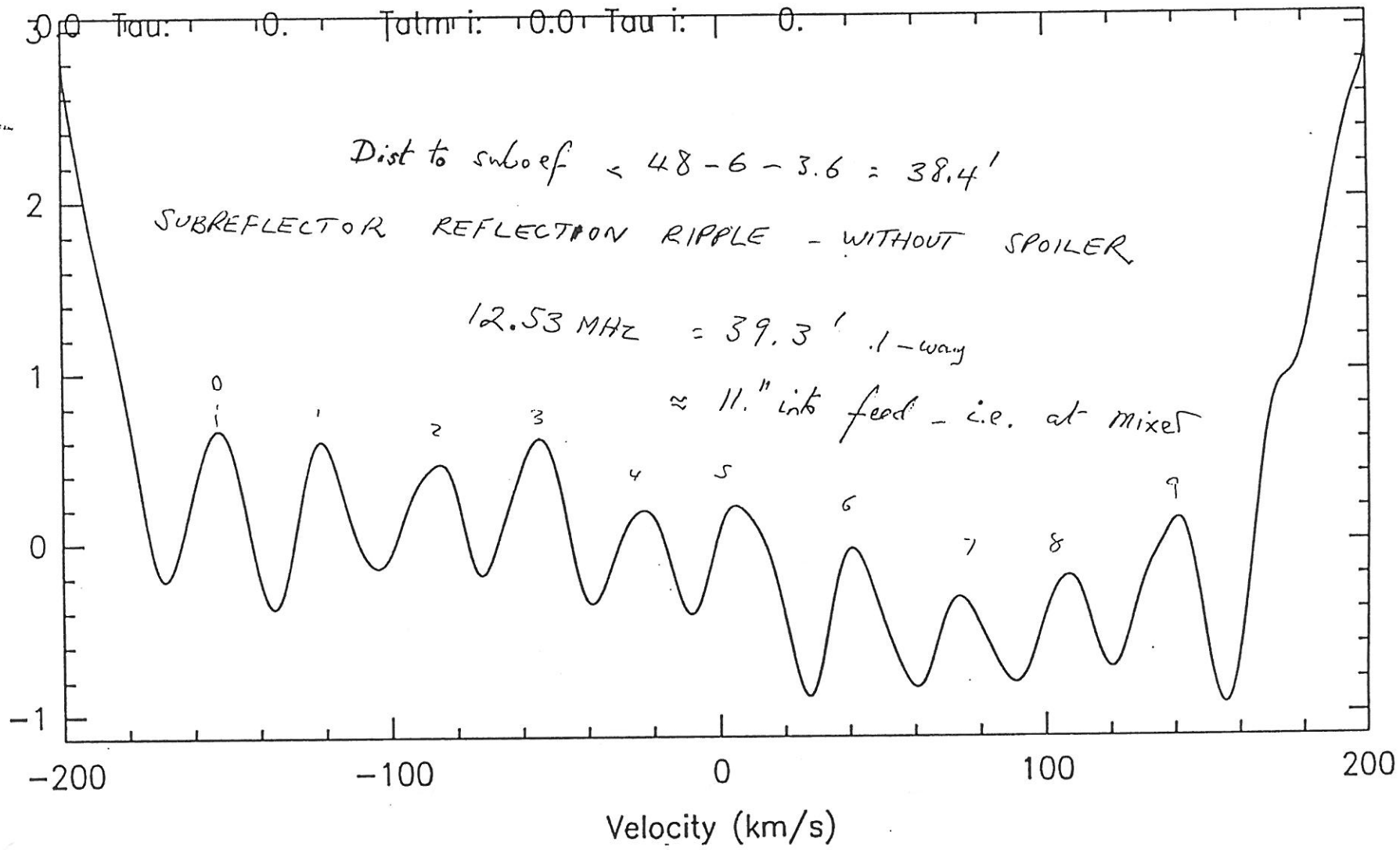


FIGURE 1. Subreflector reflection ripple - without spoiler.

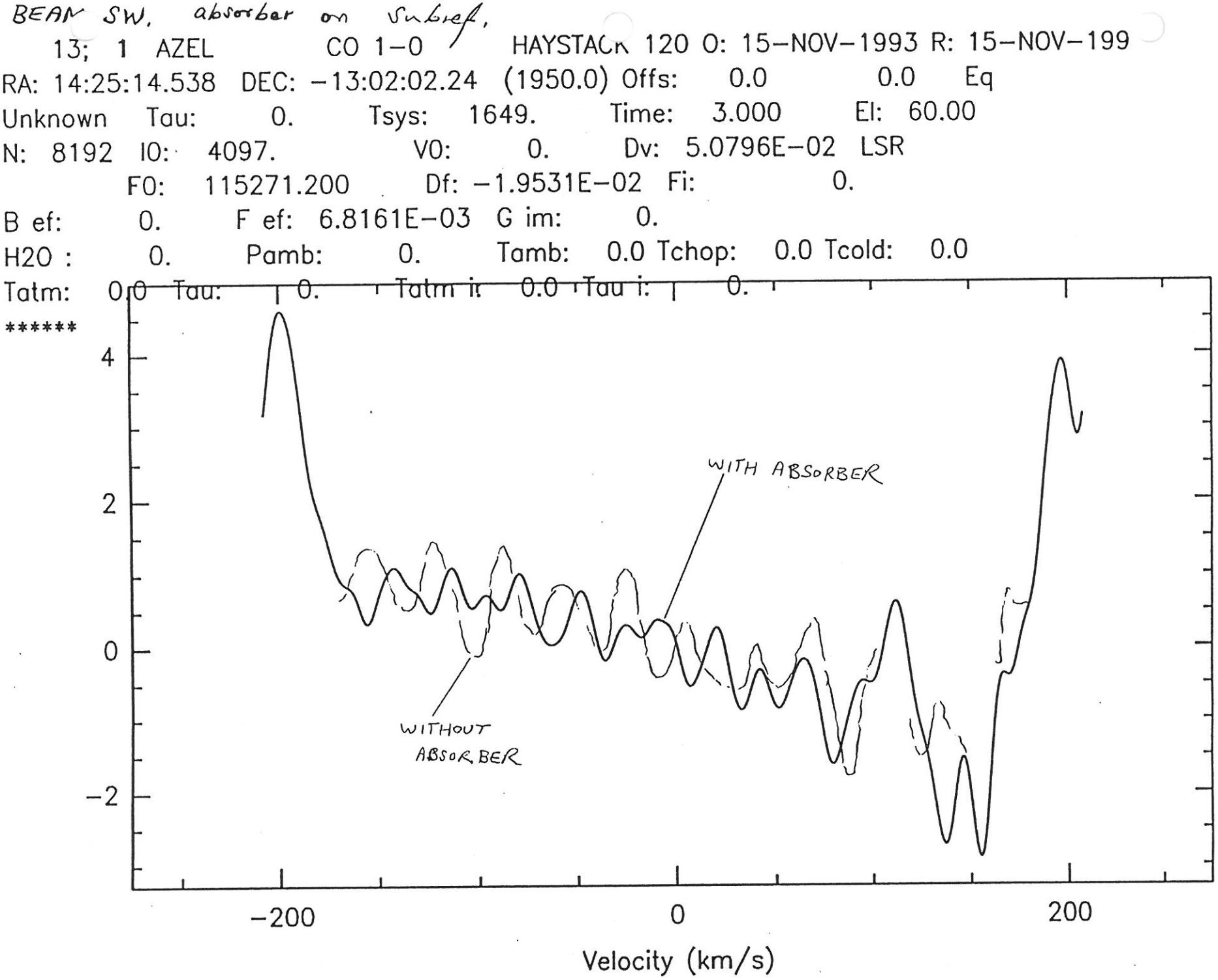


FIGURE 2. Reduction in ripple with absorber.

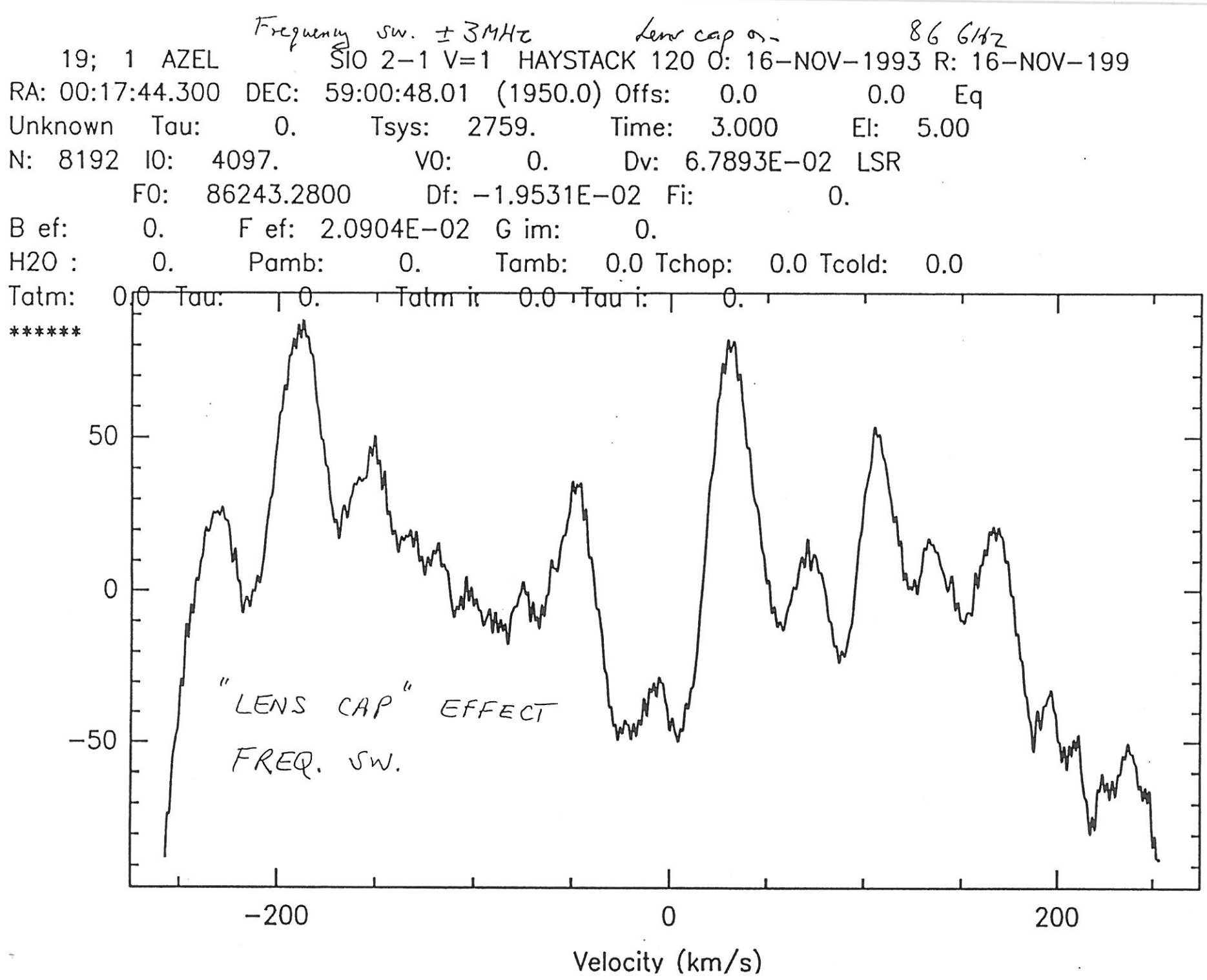


FIGURE 3. "Lens cap" effect.

30; 1 AZEL SIO 2−1 V=1 HAYSTACK 120 0.0 0.0 Eq******

90,20

86 GHz freq. sw. $T_s \approx 300\,K$

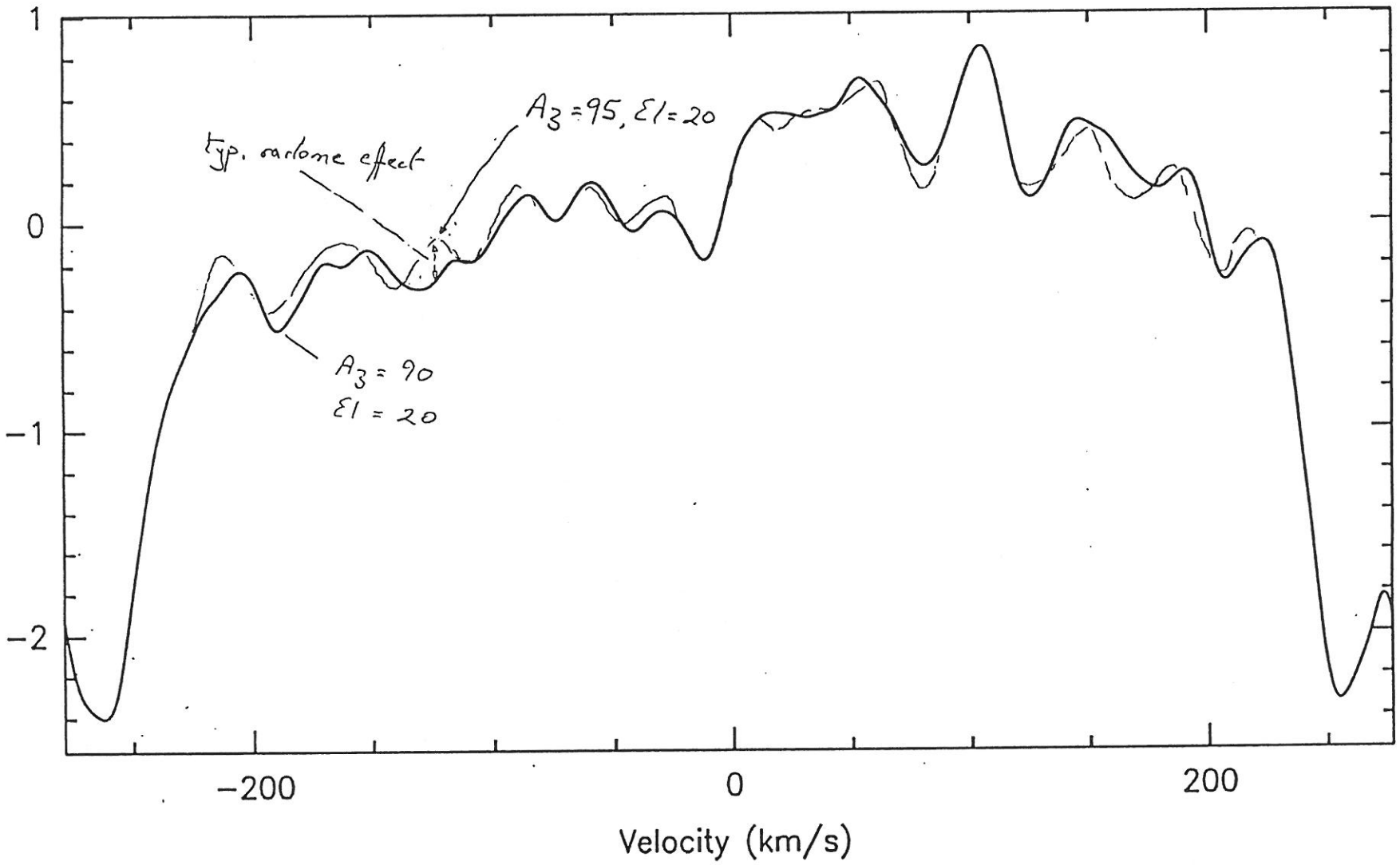


FIGURE 4. Baseline ripple at 90 and 95 degrees azimuth.

208-212 Double-Dicke

208; 1 TEST CO 1-0 HAYSTACK 120 O: 26-NOV-1993 R: 26-NOV-199

RA: 12:00:00.000 DEC: 63:00:00.00 (1950.0) Offs: 0.0 0.0 Eq

Unknown Tau: 0. Tsys: 480.5 Time: 5.000 El: 41.09

N: 31 I0: 16.00 V0: 0. Dv: 13.00 LSR

F0: 115271.200 Df: -5.000 Fi: 0.

RMS = 9.3 mK Theory r.m.s. $\frac{DD}{\left(\left(160\times10^{6}/31\right)\times60\times5\times4\times2\right)^{1/2}}$ 2 × 480 × 1.1 — 4-level = 9.5 mK

1 min/k subspectra

pairs

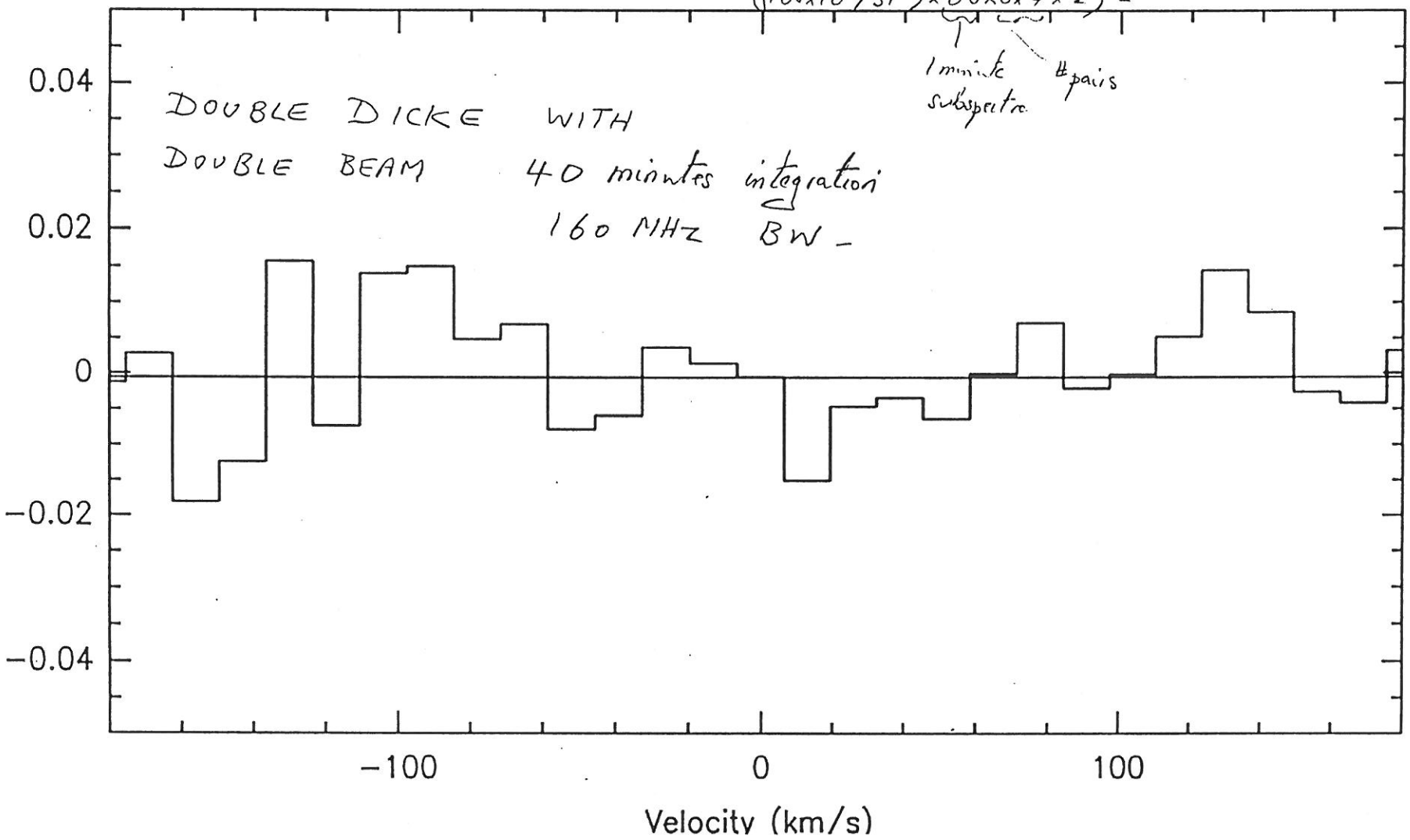
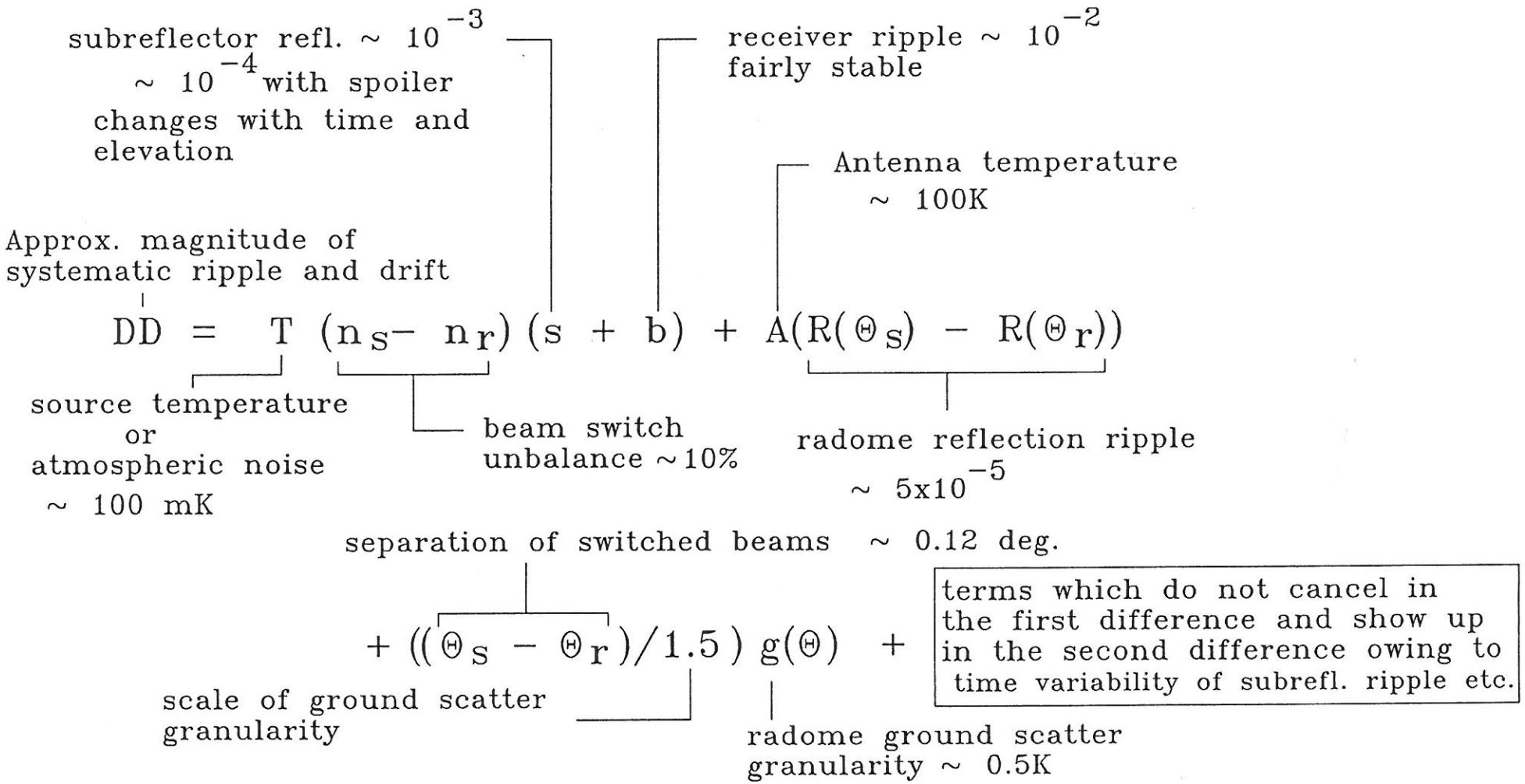


FIGURE 5. Double Dicke with double beam.



Expected limits: 1] Continuum ~ 50 mK without radome retrace
– third term dominant

2] Spectral ~ 5 mK/(# independent radome pts.obs.)$^{1/2}$
– second term dominant

Double-Dicke (double beam or radome retrace) limits for Haystack

aeer Dec 93

FIGURE 6. Summary of sensitivity limits